Acceleration of P/C-Type Inactivation in Voltage-Gated K^+ Channels by Methionine Oxidation

Jianguo Chen,* Vladimir Avdonin,* Matthew A. Ciorba,* Stefan H. Heinemann,† and Toshinori Hoshi*
*Department of Physiology and Biophysics, The University of Iowa, Iowa City, Iowa 52242 USA, and †Arbeitsgruppe Molekulare und zelluläre Biophysik am Klinikum der Friedrich-Schiller-Universität Jena, D-07747 Jena, Germany

ABSTRACT Oxidation of amino acid residues causes noticeable changes in gating of many ion channels. We found that P/C-type inactivation of Shaker potassium channels expressed in *Xenopus* oocytes is irreversibly accelerated by patch excision and that this effect was mimicked by application of the oxidant H_2O_2, which is normally produced in cells by the dismutase action on the superoxide anion. The inactivation time course was also accelerated by high concentration of O_2. Substitution of a methionine residue located in the P-segment of the channel with a leucine largely eliminated the channel's sensitivity to patch excision, H_2O_2, and high O_2. The results demonstrate that oxidation of methionine is an important regulator of P/C-type inactivation and that it may play a role in mediating the cellular responses to hypoxia/hyperoxia.

INTRODUCTION

Oxidation of amino acid residues in proteins is known to alter their functional properties (Stadtman, 1993). Ion channel proteins are often a target of oxidation induced by a diverse array of physiological factors, including those oxidants involved in intracellular signaling, such as nitric oxide (NO) (Suzuki et al., 1997; Wolin and Mohazzab, 1997; Kourie, 1998). Oxidation of amino acid residues may also mediate the sensitivity of some ion channels to oxygen (López-Barneo, 1996). Voltage-gated K^+ channels, which play important roles in action potential generation and action potential frequency, are regulated by oxidation (Kourie, 1998). Among the cloned K^+ channels, oxidation decreases the activity of Kv1.3 (Duprat et al., 1995; Szabo et al., 1997), Kv1.4, Kv1.5, Kv3.4 (Duprat et al., 1995), and Kv3.3 (Vega-Saenz de Miera and Rudy, 1992), while outward K^+ currents through HERG channels are enhanced by oxidation (Taglialatela et al., 1997). Deactivation of the Kv1.4 channel is also slowed by oxidation (Stephens et al., 1996). N-type inactivation mediated by the ball-and-chain mechanism in Kv1.4 (RCK4) and Kv1.4/Kvβ channels is dependent on the cellular redox state in a cysteine-dependent manner (Ruppersberg et al., 1991; Rettig et al., 1994; Heinemann et al., 1995).

Methionine is readily oxidized to form methionine sulfoxide (met(O)) by the addition of an oxygen to the sulfur atom (Stadtman, 1993; Vogt, 1995). In strong oxidative conditions, met(O) can be further oxidized to methionine sulfone (Vogt, 1995). Oxidation of methionine to met(O) alters the side-chain property such that changes in the overall protein hydrophobicity may be observed (Chao et al., 1997). Physiological oxidation of methionine residues has been documented in calmodulin isolated from aged brains (Michaelis et al., 1996). Cellular reduction of met(O) to methionine is catalyzed by the enzyme peptide methionine sulfoxide reductase (MSRA) using thioredoxin (Rahman et al., 1992; Moskovitz et al., 1996). Methionine oxidation and MSRA may function as a general antioxidant mechanism (Levine et al., 1996; Moskovitz et al., 1998) and also as a regulator of cellular function (Ciorba et al., 1997; Berlett et al., 1998; Gao et al., 1998; Ciorba et al., 1999; Kuschel et al., 1999). Localization of human MSRA in some tissues, including selected regions of the brain, suggests that methionine oxidation and MSRA may have specific physiological roles (Kuschel et al., 1999). Methionine oxidation has been shown to modulate N-type inactivation of a *Drosophila* transient A-type K^+ channel (ShC/B) expressed in oocytes (Ciorba et al., 1997). Oxidation of methionine at position 3 in the cytoplasmic inactivation ball domain to met(O) dramatically slows down inactivation, and heterologous expression of MSRA accelerates the inactivation time course. Nitric oxide, possibly working via peroxynitrite, also slows down the ShC/B inactivation time course by promoting oxidation of the N-terminal methionine (Ciorba et al., 1999).

In the absence of N-type inactivation, the Shaker channel displays P/C-type inactivation (Hoshi et al., 1991; Cha and Bezanilla, 1997; Olcese et al., 1997; Loots and Isacoff, 1998). P/C-type inactivation is mediated at least in part by the amino acid residues in the S5-, P-, and S6-segments of the channel (Iverson and Rudy, 1990; Hoshi et al., 1991; López-Barneo et al., 1993; Heginbotham et al., 1994; Olcese et al., 1997; Yang et al., 1997; Ogielska and Aldrich, 1998; Ogielska and Aldrich, 1999). In the ShB channel, for example, both residue 449 in the external mouth of the P-segment and residue 463 in the S6 segment control P/C-type inactivation, although residue 449 appears to have a more dominating influence over residue 463 (Hoshi et al., 1991; López-Barneo et al., 1993; Ogielska and Aldrich, 1999). P/C-type inactivation is considered to involve con-

Received for publication 30 June 1999 and in final form 21 September 1999.

Address reprint requests to Dr. Toshinori Hoshi, Department of Physiology and Biophysics, Bowen 5660, The University of Iowa, Iowa City, IA 52242. Tel.: 319-335-7845; Fax: 319-353-5541; E-mail: hoshi@physiology.uiowa.edu.

0006-3495/00/01/174/14 $2.00

striction of the ion conduction pathway (Yellen et al., 1994; Liu et al., 1996; Schlief et al., 1996), and P- and C-type inactivation mechanisms could be distinguished by using different experimental protocols (Cha and Bezanilla, 1997; Meyer and Heinemann, 1997; Olcese et al., 1997; Loots and Isacoff, 1998). It has been suggested that the channel first enters the relatively unstable P-type inactivated state and then proceeds to enter the more stable C-type inactivated state (Loots and Isacoff, 1998). Like N-type inactivation, P/C-type inactivation may be regulated by cytoplasmic factors as patch excision alters the inactivation time course in the Kv1.3 channel (Kupper et al., 1995). Those Shaker channels with fast P/C-type inactivation are also known to be more sensitive to the oxidizing agent chloramine-T (Ch-T) (Schlief et al., 1996).

The Shaker potassium channel contains multiple methionine residues at various locations, including the P-segment. Because many residues in the P-segment are known to be involved in regulation of P/C-type inactivation (Iverson and Rudy, 1990; Hoshi et al., 1991; López-Barneo et al., 1993; Olcese et al., 1997; Yang et al., 1997; Ogielska and Aldrich, 1998), we examined how methionine oxidation may regulate P/C-type inactivation in the absence of N-type inactivation. The results show that oxidation of a specific methionine residue in the Shaker channel P-segment modulates the inactivation time course and that oxidation of this methionine is promoted by high O_2, suggesting that methionine oxidation may play a role in the regulation of cellular excitability in response to hypoxia/hyperoxia.

MATERIALS AND METHODS

Mutant channel

The ShBΔ6–46:M440L:T449S plasmid DNA was constructed by standard polymerase chain reaction-mediated cassette mutagenesis, using the *Hin*dIII and *Nsi*I sites in the ShBΔ6–46 DNA (López-Barneo et al., 1993). The fragment amplified by polymerase chain reaction was sequenced (The University of Iowa DNA core).

Expression in oocytes

The K^+ channels were expressed in *Xenopus* oocytes essentially as described previously (Hoshi et al., 1990), using an animal use protocol approved by the University of Iowa Animal Care and Use Committee. The ShBΔ6–46:T449S, ShBΔ6–46:T449K, and ShBΔ6–46:M440L:T449S DNAs were linearized with *Nde*I, and the RNAs were synthesized with T7 RNA polymerase, using a commercially available kit (Ambion, Austin, TX). Recombinant purified bovine MSRA (Moskovitz et al., 1996) was obtained from N. Brot (Hospital for Special Surgery, New York, NY).

Electrophysiology

The patch-clamp recordings were obtained with an AxoPatch 200 amplifier (Axon Instruments, Foster City, CA). The borosilicate pipettes were coated with dental wax to record macroscopic currents and with sylgard to record single-channel currents. Unless otherwise indicated, the holding voltage was −90 mV. Because of the slow recovery from inactivation of the ShBΔ6–46:T449S channel, depolarizing pulses were applied every 60 s, which severely hindered the single-channel data collection. The patch-clamp output signal was filtered through a Bessel filter unit and digitized with an ITC-16 interface (Instrutech, Port Washington, NY) attached to an Apple Power Macintosh computer. The macroscopic currents were filtered at 3 kHz, and the single-channel currents were filtered at 5 kHz. The single-channel data were further filtered digitally for later analysis. The data were collected and analyzed using Pulse/PulseFit (HEKA, Lambrecht, Germany), PatchMachine (http://www.hoshi.org), IgorPro (WaveMetrics, Lake Oswego, OR), and DataDesk (DataDescriptions, Ithaca, NY). Linear leak and capacitative currents have been subtracted from the data presented.

The macroscopic inactivation time course was fitted with a single exponential or the sum of two exponentials using IgorPro, excluding the initial 3.5 ms after the depolarization onset. The rate constant values in the three-state scheme presented (Scheme II; see later) were also estimated using IgorPro. The single-channel analysis was performed using PatchMachine (http://www.hoshi.org) and custom routines implemented in IgorPro (Avdonin et al., 1997).The normal external/pipette solution contained (in mM) 140 NaCl, 10 KCl, 2 $CaCl_2$, and 10 HEPES, with the pH adjusted to 7.2 with *N*-methylglucamine (NMG). The high K^+ external/pipette solution contained (in mM) 10 NaCl, 140 KCl, 2 $CaCl_2$, and 10 HEPES, with the pH adjusted to 7.2 with NMG. The internal/bath solution contained (in mM) 140 KCl, 2 $MgCl_2$, 10 EGTA, and 10 HEPES, with the pH adjusted to 7.2 with NMG. In the presence of this high K^+ solution, after the vitelline membrane removal, the oocytes had a typical resting potential of ~0 mV, as verified by an intracellular microelectrode filled with 3 M KCl (data not shown). Thus the absolute voltages in the cell-attached and inside-out configurations are expected to be very similar.

H_2O_2 (Sigma, St. Louis, MO) solutions were prepared immediately before use. For the high-O_2 experiments, the bath solution was aerated with 100% O_2 for at least 20 min before use.

RESULTS

Variability in the ShBΔ6–46:T449S inactivation time course

The ShBΔ6–46:T449S channel contains a large deletion in the N-terminus (Δ6–46) to disrupt N-type inactivation mediated by the ball-and-chain mechanism (Hoshi et al., 1990). The T449S mutation in the P-segment accelerates the P/C-type inactivation time course to a more experimentally manageable range (López-Barneo et al., 1993; Schlief et al., 1996; Meyer and Heinemann, 1997). Representative macroscopic ShBΔ6–46:T449S currents recorded from 17 different patches in the cell-attached configuration are shown in Fig. 1. The inactivation time course of the ShBΔ6–46:T449S channel is quite fast, comparable to N-type inactivation observed in some variants of the Shaker channel (Zagotta et al., 1989). It is also clear that the inactivation time course was markedly variable in different patches. To quantify the inactivation kinetics, the current time course of the ShBΔ6–46:T449S channel was approximated by the sum of two exponential components, consistent with the earlier observation of Meyer and Heinemann that the channel undergoes two distinct inactivation phases (Meyer and Heinemann, 1997). In different patches, the time constant values were similar, ~5 and ~40 ms (see Fig. 2 *D*), but the relative amplitudes of the two exponential components were

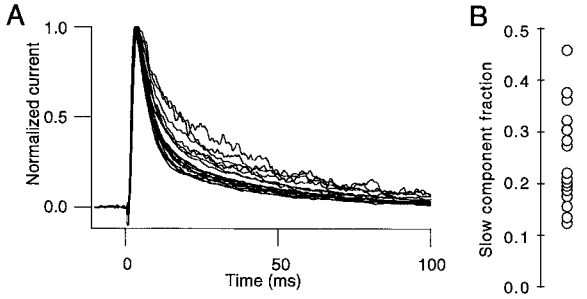

FIGURE 1 Inactivation time course of the ShBΔ6–46:T449S channel is variable. (*A*) Currents recorded in the cell-attached configuration in response to pulses from −90 mV to +50 mV are scaled and shown superimposed. The data were obtained from multiple oocytes isolated from one animal. The mean peak amplitude of the currents shown was 1.3 (± 0.4) nA. The Spearman rank correlation rho between the peak current amplitude and the relative amplitude of the slow inactivation component was −0.57. (*B*) The current traces shown in *A* were fitted with the sum of two exponential functions, and the relative amplitudes of the slow inactivation component in the patches examined are shown. The time constant values are shown in Fig. 2 *D*.

noticeably different, with the slow component fraction ranging from 10% to 50% (Fig. 1 *B*). This inactivation variability was even present in multiple patches taken from the same oocyte. The observed variability indicates that the inactivation process is subject to biological regulation. N-type inactivation of the ShC/B channel expressed in *Xenopus* oocytes also shows similar variability, and methionine oxidation has been shown to underlie this variability (Ciorba et al., 1997).

Patch excision accelerates the inactivation time course

Patch excision is known to influence inactivation of several heterologously expressed voltage-dependent K^+ channels, including Kv1.4 (Ruppersberg et al., 1991), Kv1.4/Kvβ (Rettig et al., 1994; Heinemann et al., 1995), Kv1.3 (Kupper et al., 1995), Raw3 (Kv3.4) (Ruppersberg et al., 1991), and ShC/B (Ciorba et al., 1997). These observations have been interpreted to suggest that the channels are regulated by cytoplasmic factors. Oxidative modifications of cysteine and methionine account for the changes in N-type inactivation induced by patch excision in Kv1.4 (Ruppersberg et al., 1991), Kv1.4/Kvβ (Rettig et al., 1994; Heinemann et al., 1995), and ShC/B (Ciorba et al., 1997), respectively. We found that the inactivation time course of the ShBΔ6–46:T449S channel that displays only P/C-type inactivation was accelerated by patch excision. Fig. 2 *A* compares representative ShBΔ6–46:T449S currents recorded from one patch in the cell-attached and the excised configurations. Patch excision markedly accelerated the overall inactivation time course. The inactivation time course was fitted with the sum of two exponentials, and the time constant values and the relative amplitudes of the two exponential components are

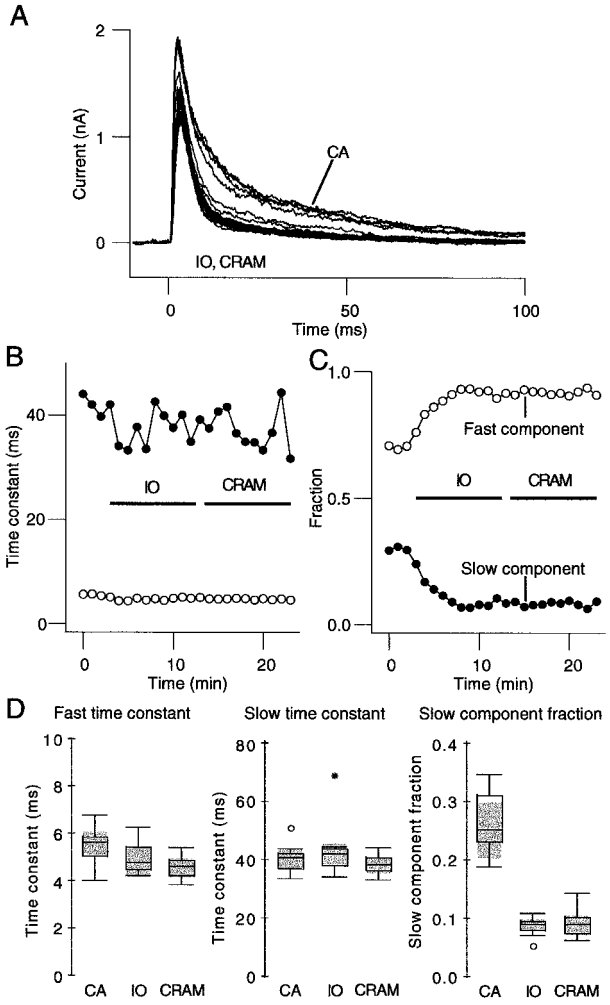

FIGURE 2 Patch excision accelerates the ShBΔ6–46:T449S channel inactivation. (*A*) Consecutive currents recorded in response to pulses from −90 mV to +50 mV in the cell-attached (CA), inside-out (IO), and cramming (CRAM) configurations in one representative experiment. The current traces recorded in the cell-attached configuration were slower than those in the inside-out or cramming configuration. (*B*) The currents traces shown in *A* were fitted with the sum of two exponentials, and the time constant values in the three patch-clamp configurations, as indicated by the horizontal bars, are plotted. The time constant values were not affected by the patch configuration. (*C*) Relative amplitudes of the two exponential components in the three patch-clamp configurations. The current traces in *A* were fitted with the sum of two exponentials. The relative amplitude of the slow inactivation component is smaller in the inside-out and cramming configurations, and patch-cramming did not restore the fractional amplitude. (*D*) Comparison of the inactivation fit parameters in the cell-attached, inside-out, and cramming configurations. Currents traces from multiple patches (n = 10) were fitted with the sum of two exponentials, and the inactivation parameters in different configurations are shown using box plots (Velleman and Hoaglin, 1981). Briefly, the central box represents the middle 50% of the data, and the center line shows the median. The whiskers show the main body of the data, excluding outliers. The shaded area represents the 95% confidence interval of the median. The difference in the slow component fraction between the cell-attached and inside-out configurations is significant at p = 0.002 (paired sign test).

plotted as a function of time in the experiment in Fig. 2, *B* and *C*. The results show that patch excision noticeably decreased the fractional amplitude of the slow inactivation component without markedly affecting the time constant values of the two components. Patch cramming, where the electrode tip is inserted back into the oocyte cytoplasm to expose the channels to the cytoplasmic factors (Kramer, 1990), did not restore the inactivation time course of the ShBΔ6–46:T449 channel (Fig. 2, *B* and *C*). The effect by patch excision of accelerating the inactivation kinetics was complete within 5–10 min. The inactivation parameters pooled from multiple patches are compared in Fig. 2 *D*, using box plots. The comparison again shows that patch excision did not markedly affect the time constant values, but it specifically decreased the relative amplitude of the slow inactivation component ($p = 0.002$, paired sign test). Although patch excision significantly decreased the relative fraction of the slow component, it did not totally eliminate it, typically leaving 5–10%. These results indicate that patch excision destroys or exhausts the factors necessary to keep the P/C-type inactivation time course slow and that regeneration of those factors in the oocyte cytoplasm is very slow. The changes in the inactivation time course observed (Fig. 2 *A*) are also reminiscent of the inactivation variability observed in different patches (Fig. 1 *A*) in that the relative fraction of the slow inactivation component is preferentially altered, suggesting that the same mechanism may underlie these phenomena.

Patch excision decreases the mean open and burst durations

We examined the effects of patch excision at the single-channel level, and the results from a representative experiment are shown in Fig. 3. In the cell-attached configuration, several bursts of openings are observed late in the pulse ($t >$ 25 ms). After patch excision, multiple bursts were rarely observed in a single sweep, and no openings were found at $t > 25$ ms. The results obtained from multiple single-channel patches ($n = 6$) show that patch excision decreased the mean open duration from 2.4 ms to 1.7 ms ($p < 0.001$, Wilcoxon signed rank test). The burst analysis using 9 ms as the burst criterion, which considers both the C_f and C_i closed events (Hoshi et al., 1994) as intraburst events, showed that patch excision also decreased the mean burst duration from 15 to 6.5 ms ($p \leq 0.0001$, Wilcoxon signed rank test). The decrease in the mean open and burst durations indicates that patch excision destabilizes the states involved in the channel's burst behavior. Consistent with the macroscopic results, the decay of the ensemble average current became noticeably faster on patch excision (Fig. 3 *B*). To record the single-channel current data, depolarization pulses were applied every 60 s because of the slow recovery from inactivation, making collection of the first latency data difficult. Thus we pooled the first latency data collected from multiple single-channel patches in the cell-attached and inside-out configurations, and the resulting distributions are compared in Fig. 3 *C*. The first latency distributions are statistically indistinguishable (Kolmogorov-Smirnov test,

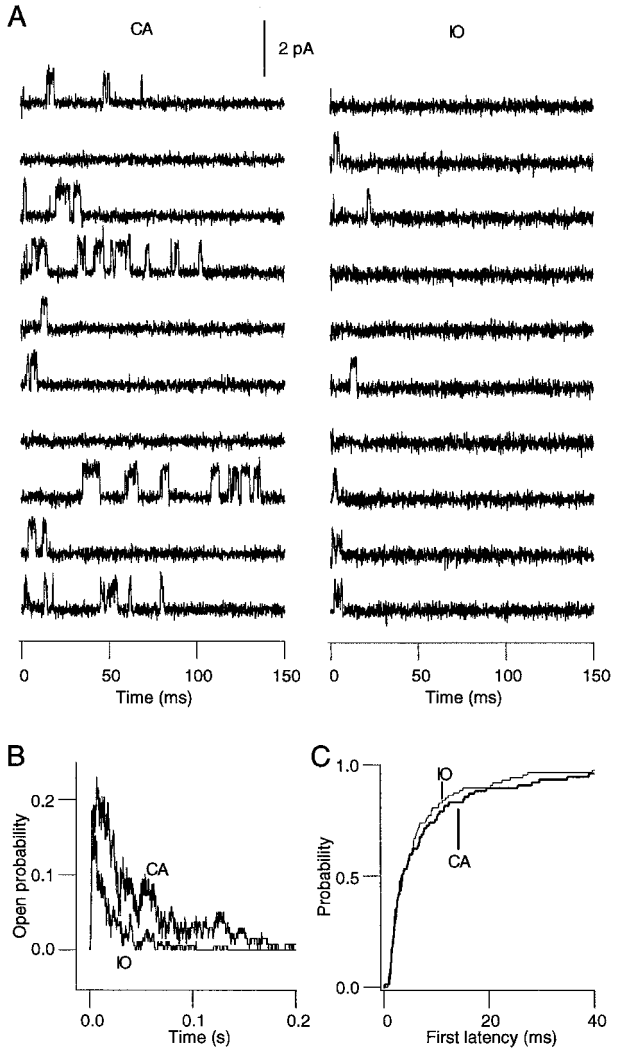

FIGURE 3 Patch excision inhibits late single-channel openings. (*A*) Representative single channel records obtained in the cell-attached (*left*) and inside-out (*right*) configurations. The openings were elicited by pulses from −100 mV to 0 mV every 60 s. After the sweeps shown in the left panel were collected, the patch was excised. The data shown in the right panel were collected 10 min after the patch excision. The records shown are consecutive sweeps recorded. The records shown were digitally low-pass filtered at 2 kHz. (*B*) Ensemble averages obtained from idealized single-channel openings recorded at 0 mV in the cell-attached and inside-out configurations. Data from six single-channel patches were pooled because it was not practical to obtain a large number of sweeps from one patch because of the slow recovery from inactivation. (*C*) The first latency distributions obtained in the cell-attached (*thick line*) and inside-out (*thin line*) configurations. The channel openings are elicited as in *A*. Each distribution shows the probability that the channel has opened by the time indicated on the *x* axis, given that there was at least one opening in the record. Data from six single-channel patches containing 57 and 61 first latency events in the cell-attached and inside-out configurations are pooled.

$p > 0.2$), confirming that patch excision directly affected the inactivation mechanisms. These single-channel results thus suggest that individual ShBΔ6–46:T449S channels are capable of showing both fast and slow inactivation patterns and that patch excision promotes the fast inactivation mode. These single-channel results are consistent with the results of an earlier thermodynamics study, in which this channel shows two distinguishable inactivation components (Meyer and Heinemann, 1997). The results also argue against the possibility that those channels showing slow inactivation preferentially disappear on patch excision.

Analysis using three-state models

Because a given channel is capable of showing both fast and slow inactivation components, the double-exponential macroscopic inactivation time course in the ShBΔ6–46:T449S channel could be interpreted in the following two ways:

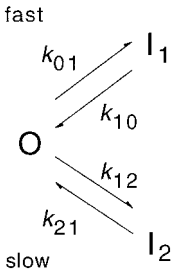

Scheme1

$$O \underset{k_{10}}{\overset{k_{01}}{\rightleftharpoons}} I_1 \underset{k_{21}}{\overset{k_{12}}{\rightleftharpoons}} I_2$$

Scheme 2

In Scheme I, the channel enters two distinct inactivated states in a mutually exclusive manner. The O-I_1 and O-I_2 pathways in Scheme I account for the fast and slow inactivation components in the macroscopic inactivation time course of the ShBΔ6–46:T449S channel, respectively (Fig. 2). With this interpretation, the results in Fig. 2 *C* indicate that patch excision causes the channel to inactivate via the O-I_1 pathway more frequently by increasing the relative value of k_{01} over that of k_{12}. Based on the relative amplitudes of the two macroscopic inactivation components, in the cell-attached configuration, the probability of the channel inactivating via the slow O-I_2 pathway is ~0.3, and patch excision decreases the probability to less than 0.1.Alternatively, in Scheme II, the channel sequentially enters two kinetically distinct inactivated states. Scheme II is consistent with the observation that, in the absence of N-type inactivation, the Shaker channel may first enter the relatively unstable P-type inactivated state and then the more stable C-type inactivated state (Loots and Isacoff, 1998). According to this interpretation, the I_1 state may represent the P-type inactivated state and the I_2 state may represent the C-type inactivated state. The results from macroscopic current data presented below were analyzed using Scheme II as the framework, which in turn is consistent with the results of Loots and Isacoff (1998) that the channel sequentially enters P- and then C-type inactivated states. The Scheme II rate constant values in the cell-attached, inside-out, and cramming configurations from one representative patch are shown in Fig. 4 *A*. Patch excision increased the value of k_{01} by ~100% from 150 s^{-1} to 300 s^{-1} and decreased the value of k_{10} by 50% from ~40 s^{-1} to ~20 s^{-1}. The k_{12} and k_{21} values were not noticeably affected by patch excision. Furthermore, patch cramming did not affect any of the rate constants. The rate constant values estimated from multiple patches are compared in Fig. 4 *B*, showing again that only k_{01} and k_{10} are noticeably affected by patch excision. The increase in k_{01} is consistent with the single-channel results that patch excision decreased the mean burst duration. Using the interpretation of the double-exponential inactivation time course presented above, this kinetic analysis suggests that the kinetic transitions between the open and the P-type inactivated states are preferentially affected by patch excision.

High external K^+ does not alter the sensitivity to patch excision

High external K^+ slows entry into P/C-type inactivation by preventing clearance of ions from the channel pore (López-Barneo et al., 1993; Baukrowitz and Yellen, 1995; Levy and Deutsch, 1996; Starkus et al., 1997). We examined whether high K^+ influences the acceleration of the inactivation time course of the ShBΔ6–46:T449S channel induced by patch excision. The ShBΔ6–46:T449S currents were recorded in the presence of 140 mM extracellular K^+. As shown in other ShBΔ6–46 channels without N-type inactivation (López-Barneo et al., 1993), high external K^+ slowed the overall inactivation time course of the ShBΔ6–46:T449S channel. The double-exponential nature of the inactivation time course observed with low K^+ was maintained in the presence of 140 mM extracellular K^+. The inactivation time constant values were approximately twice as great as those found with low K^+, and the relative fraction of the slow inactivation was also greater with high K^+, ranging from 30% to 60% in the cell-attached configuration (cf. Fig. 2). In the presence of high external K^+, patch excision still accelerated the inactivation time course most noticeably by decreasing the relative fraction of the slow inactivation component (Fig. 5, *B* and *C*). A small decrease in the time constant value of the slow component was also observed. The currents recorded in the cell-attached and inside-out configurations using low external K^+ and high external K^+ are scaled and compared in Fig. 5 *D*. High external K^+ slowed the inactivation time course in both the cell-attached and inside-out configurations in a qualitatively similar man-

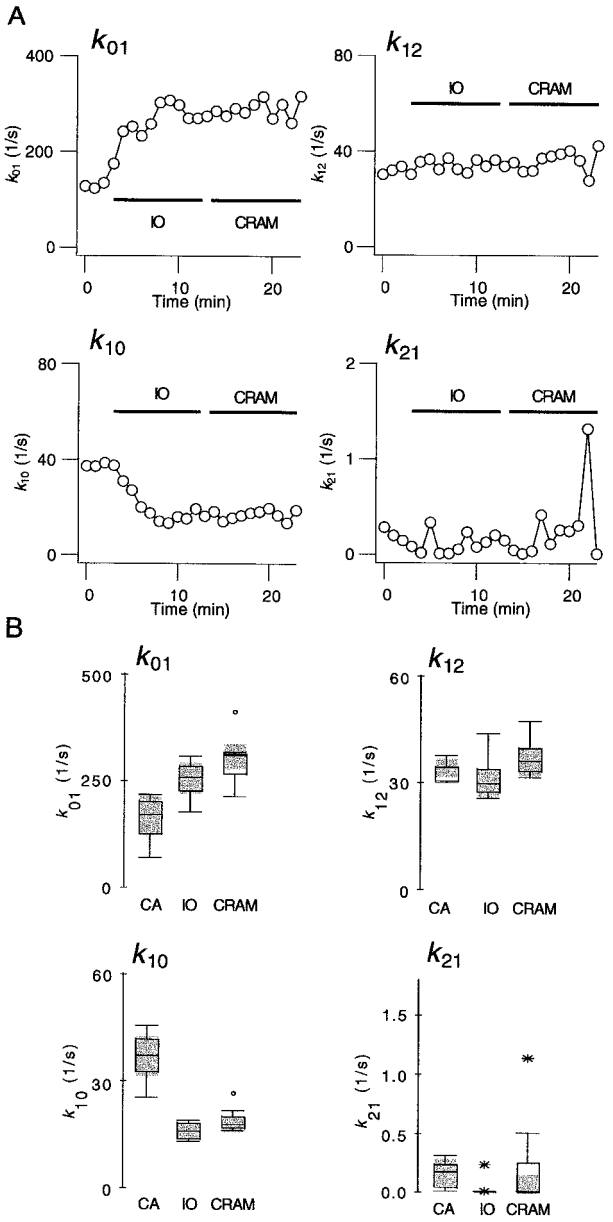

FIGURE 4 Patch excision alters the rate constants near the open state. (*A*) Currents traces shown in Fig. 2 *A* were fitted with the three-state model (Scheme II; see text), and the rate constant values estimated in the three patch-clamp configurations, as indicated by the horizontal bars, are plotted. (*B*) Comparison of the values of the rate constants in the three-state model (Scheme II; see text) in the cell-attached, inside-out, and cramming configurations in multiple patches. The results from 10 different patches are compared using box plots. The differences in k_{01} and k_{10} between the cell-attached and inside-out configurations are significant at $p = 0.002$ and 0.002, respectively (paired sign test).

ner, suggesting that patch excision does not influence the inactivation time course by regulating its external K^+ sensitivity. The results obtained with high external K^+ were also analyzed using Scheme II (Fig. 5 *E*). As found using low external K^+, patch excision markedly increased the value of k_{01} and decreased the value of k_{10}.

We also estimated the time courses of recovery from inactivation in the cell-attached and inside-out configurations, using a standard double-pulse protocol. We found that the recovery kinetics was not affected by patch excision at −90 mV ($n = 5$; data not shown).

Hydrogen peroxide accelerates the inactivation time course

Cellular reduction of met(O) to methionine is catalyzed by MSRA (Rahman et al., 1992; Moskovitz et al., 1996; Kuschel et al., 1999). Because oocytes have a low level of MSRA activity (Ciorba et al., 1997), the effect of methionine oxidation on channel function is expected to be essentially irreversible without exogenous MSRA. The observation that the effect of patch excision is not reversed by patch cramming is consistent with the idea that oxidation of methionine might be involved in regulation of the P/C-type inactivation time course of the ShBΔ6–46:T449S channel by patch excision described above. Hydrogen peroxide (H_2O_2) is normally produced in cells by the action of the dismutase on the superoxide anion ($O_2^{\bullet -}$) (Chance et al., 1979; Wolin and Mohazzab, 1997), and it has been used widely to induce oxidation in many different experimental systems (Vega-Saenz de Miera and Rudy, 1992; Wang et al., 1996; Kourie, 1998). H_2O_2 is capable of oxidizing methionine to met(O) (Vogt, 1995; Keck, 1996). Thus we attempted to determine whether H_2O_2 could mimic the effect of patch excision to accelerate the inactivation time course of the ShBΔ6–46:T449S channel by decreasing the fractional amplitude of the slow inactivation component. Representative currents recorded in the cell-attached configuration before and after addition of H_2O_2 are shown in Fig. 6. H_2O_2 (0.03–0.1%) accelerated the overall inactivation time course. The H_2O_2 concentration required to accelerate the inactivation time course and the effect latency were variable in the different oocytes examined. In some patches, 0.03% H_2O_2 immediately accelerated the inactivation time course, while in others 0.1% H_2O_2 accelerated the time course only after a few minutes of incubation. This variability may reflect different oxidant scavenging capabilities of different oocytes. We also monitored the reversal potential of the macroscopic current and found that H_2O_2 did not affect the reversal potential, suggesting that the ion selectivity of the channel was unaltered by H_2O_2 (data not shown). The effect of H_2O_2 was not reversed by washing the bath with H_2O_2-free solution for up to 10 min ($n = 3$; data not shown). As observed with patch excision, H_2O_2 also accelerated the ShBΔ6-46:T449S currents in the presence of high external K^+ ($n = 4$; data not shown).

The effect of H_2O_2 was analyzed by fitting the macroscopic current time course with the sum of two exponentials. As found with patch excision, H_2O_2 accelerated the overall inactivation time course by decreasing the fractional amplitude of the slow inactivation component without

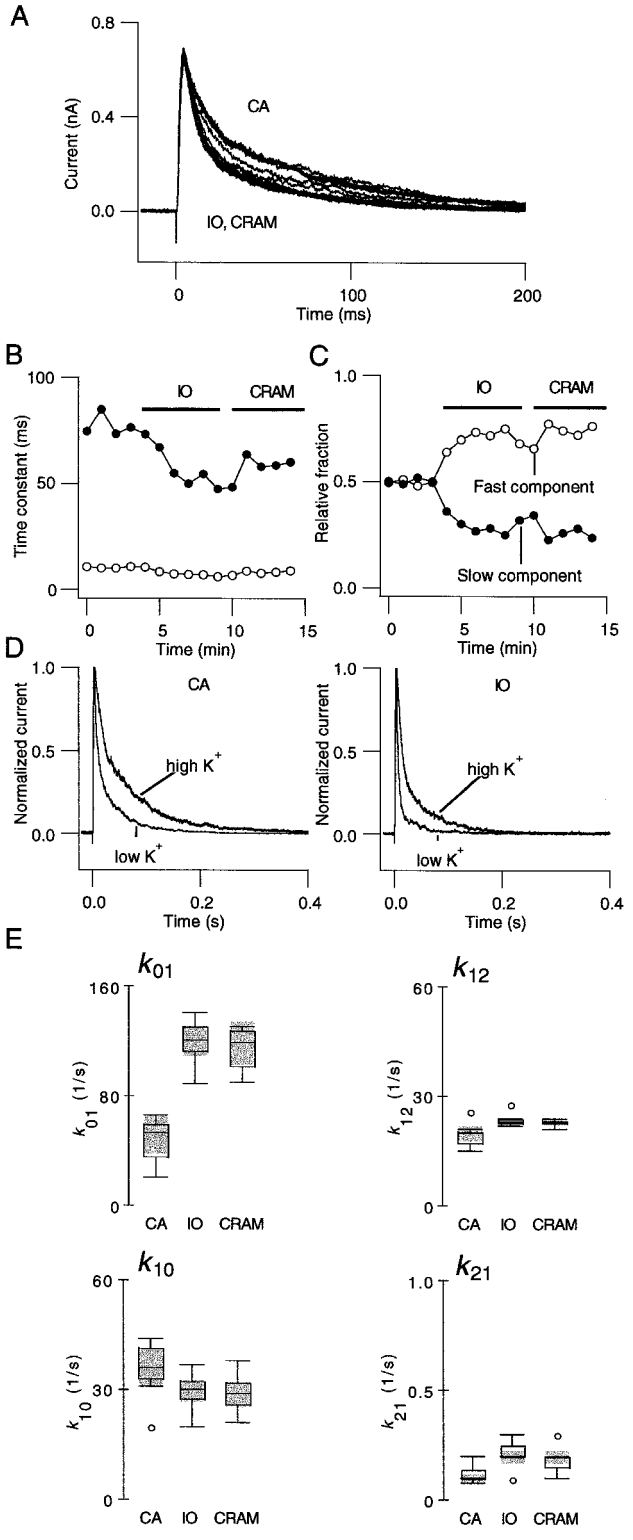

FIGURE 5 Patch excision accelerates the ShBΔ6–46:T449S inactivation time course in high external K^+. (*A*) Consecutive currents recorded in response to pulses from −90 mV to +50 mV in the cell-attached (CA), inside-out (IO), and cramming (CRAM) configurations in one representative experiment in the presence of 140 mM K^+ in the extracellular medium. The current traces recorded in the cell-attached configuration were slower than those in the inside-out or cramming configurations. (*B*) The currents traces shown in *A* were fitted with the sum of two exponentials, and the time constant values in the three patch-clamp configurations, as indicated by the horizontal bars, are plotted. (*C*) Relative amplitudes of the two exponential components in the three patch-clamp configurations. The current traces in *A* were fitted with the sum of two exponentials. The relative amplitude of the slow inactivation component is smaller in the inside-out and cramming configurations. (*D*) Scaled currents recorded at +50 mV in the cell-attached and inside-out configurations in the presence of low external K^+ (10 mM) and high external K^+ (140 mM) are shown. The left panel shows the currents recorded in the cell-attached configuration (CA), and the right panel shows the currents recorded after patch excision (IO). In each panel, the data shown are from two separate experiments, one using low K^+ and the other high K^+. (*E*) Comparison of the values of the rate constants in the three-state model (Scheme II; see text) in the cell-attached, inside-out, and cramming configurations in multiple patches. The results from seven different patches are compared using box plots.

markedly affecting the time constant values (Fig. 6 *B*). The analysis using Scheme II also shows that H_2O_2 application increased the value of k_{01} and decreased the value of k_{10} (Fig. 6 *C*; $p = 0.0078$ and 0.031, paired sign test). Thus the effects of patch excision and H_2O_2 are similar in that they both alter k_{01} and k_{10} (Fig. 4 and 6).

Hyperoxia accelerates the inactivation time course

Reactive oxygen species, such as $O_2^{\bullet -}$ and H_2O_2, are considered to be involved in cellular response to a variety of stimuli, including changes in O_2 (Suzuki et al., 1997; Wolin and Mohazzab, 1997). Therefore we attempted to determine whether high O_2 could accelerate the inactivation time course of the ShBΔ6–46:T449S channel. Representative macroscopic ShBΔ6–46:T449S currents recorded before and after the bath was perfused with the solution aerated with 100% O_2 are shown in Fig. 7. As found with H_2O_2, the high-O_2 solution markedly accelerated the overall inactivation time course by decreasing the fractional amplitude of the slow inactivation component within 5–10 min of application. Thus patch excision, H_2O_2, and O_2 affect the inactivation time course in similar ways.

ShBΔ6–46:T449K is also affected by patch excision

Position 449 in the ShB channel is one of the major determinants of P/C-type inactivation (López-Barneo et al., 1993; Schlief et al., 1996). With a lysine at this position (ShBΔ6–46:T449K), the overall inactivation time course is noticeably slower than with a serine at the same position (ShBΔ6–46:T449S) (Fig. 8; also see Schlief et al., 1996). The time course of recovery from inactivation in the ShBΔ6–46:T449K channel is also markedly faster. Kupper et al. (1995) showed that the patch excision sensitivity of Kv1.3 may be dependent on the amino acid residue present

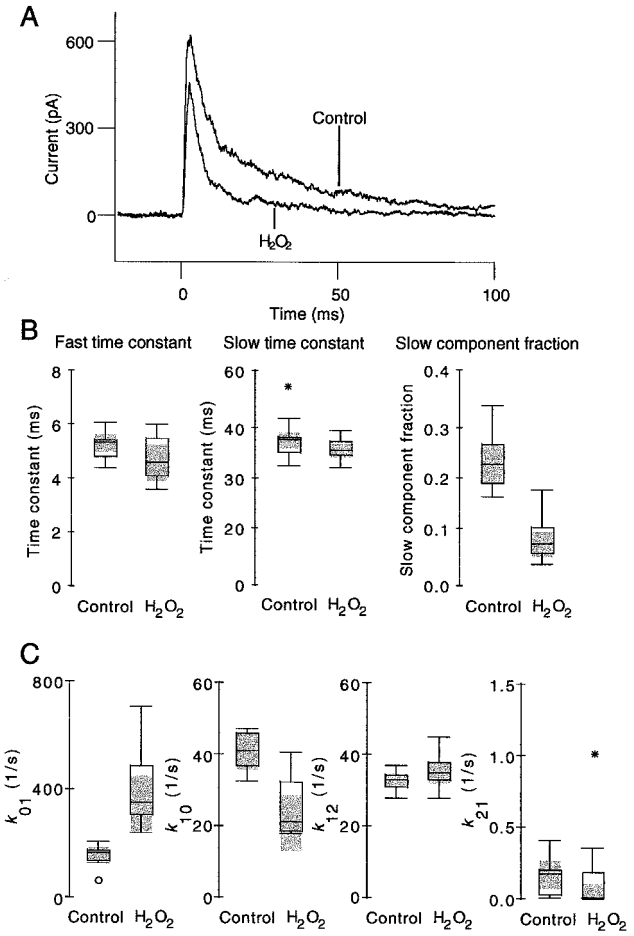

FIGURE 6 H_2O_2 accelerates the ShBΔ6–46:T449S inactivation time course. (*A*) Representative current traces recorded at +50 mV in the cell-attached configuration before and after application of H_2O_2 (0.1%). H_2O_2 was applied to the bath, and the current shown was recorded 10 min later. (*B*) Current traces before and after H_2O_2 (0.1%) from multiple patches (n = 11) were fitted with the sum of two exponentials. The fit parameters are compared using box plots. The difference in the slow inactivation fraction between the control and after H_2O_2 is significant at p = 0.001 (paired sign test). (*C*) Comparison of the values of the rate constants in the three-state model (Scheme II; see text) before and after H_2O_2 (0.1%) application. The results from 11 different patches are compared using box plots. The differences in k_{01} and k_{10} between the control and after H_2O_2 are significant at p = 0.0078 and 0.0313, respectively (paired sign test).

at the 449 equivalent position. We investigated whether the ShBΔ6–46:T449K channel was also affected by patch excision. As found with the ShBΔ6–46:T449S channel, patch excision did accelerate the overall inactivation time course of the ShBΔ6–46:T449K channel, although the effect was less pronounced (Fig. 8 *A*). Patch cramming did not restore the inactivation time course. The inactivation time course of the ShBΔ6–46:T449K channel was well approximated by a single exponential without requiring the sum of two exponentials as found in the ShBΔ6–46:T449S channel. Patch excision decreased the inactivation time constant value as compared in Fig. 8 *B*.

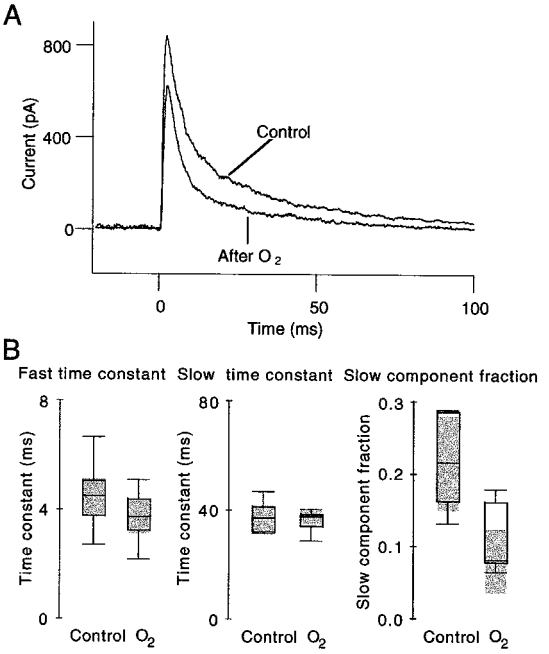

FIGURE 7 High O_2 accelerates the ShBΔ6–46:T449S inactivation time course. (*A*) Representative current traces recorded at +50 mV in the cell-attached configuration before and after application of the high O_2 bath solution. The normal bath solution, aerated with 100% O_2 for at least 20 min, was applied (three times the bath volume) every 4 min. The current shown was recorded 10 min after application of the high O_2 solution. (*B*) The current traces before and after application high O_2 solution from multiple patches (n = 9) were fitted with the sum of two exponentials. The fit parameters are compared using box plots. The difference in the slow inactivation fraction between the control and after O_2 is significant at $p \leq$ 0.0001 (paired sign test).

M440 in the P-segment may mediate the channel sensitivity to patch excision, H_2O_2, and hyperoxia

The results presented thus far suggest that patch excision, H_2O_2, and high O_2 accelerate the ShBΔ6–46:T449S inactivation time course in a kinetically similar manner, suggesting that their underlying mechanisms are common. H_2O_2 is known to oxidize methionine to met(O) (Vogt, 1995), and, in some conditions, this oxidant may specifically affect methionine (Keck, 1996). Because many residues in the S5-, P-, and S6-segments are known to affect the P/C-type inactivation time course (Iverson and Rudy, 1990; Hoshi et al., 1991; López-Barneo et al., 1993; Heginbotham et al., 1994; Schlief et al., 1996; Olcese et al., 1997; Yang et al., 1997; Ogielska and Aldrich, 1998), we hypothesized that oxidation of methionine at position 440 (M440 in ShB numbering) located in the P-segment could account for the acceleration of the inactivation time course by patch excision, H_2O_2, and high O_2. According to this hypothesis, when M440 is not oxidized the slow component of the inactivation time course is prominent, and when M440 is oxidized to met(O), the slow component fraction decreases.

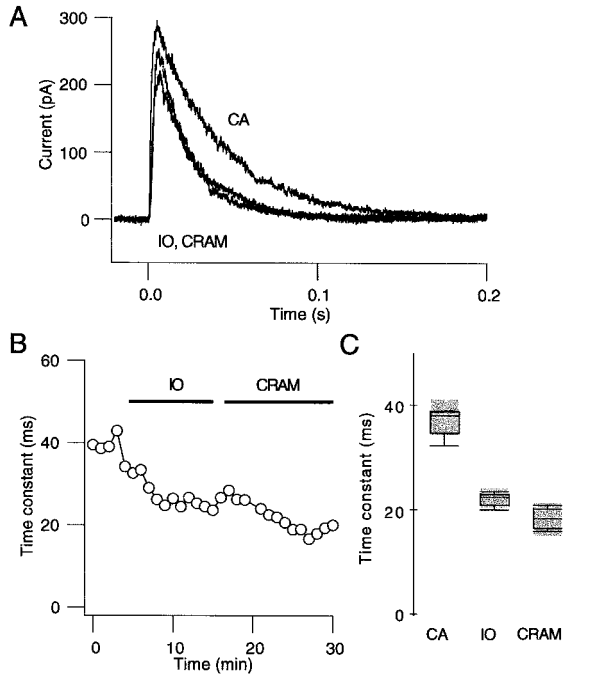

FIGURE 8 The inactivation time course of the ShBΔ6–46:T449K channel is also sensitive to patch excision. (*A*) Representative currents recorded in response to pulses from −90 mV to +50 mV in the cell-attached (CA), inside-out (IO), and cramming (CRAM) configurations in one representative experiment. (*B*) The current traces in the cell-attached (CA), inside-out (IO), and cramming (CRAM) configurations are fitted with a single exponential. The time constant values are plotted as a function of time in one representative experiment. (*C*) Time constant of inactivation measured from multiple patches (n = 4) in different patch-clamp configurations is compared using box plots.

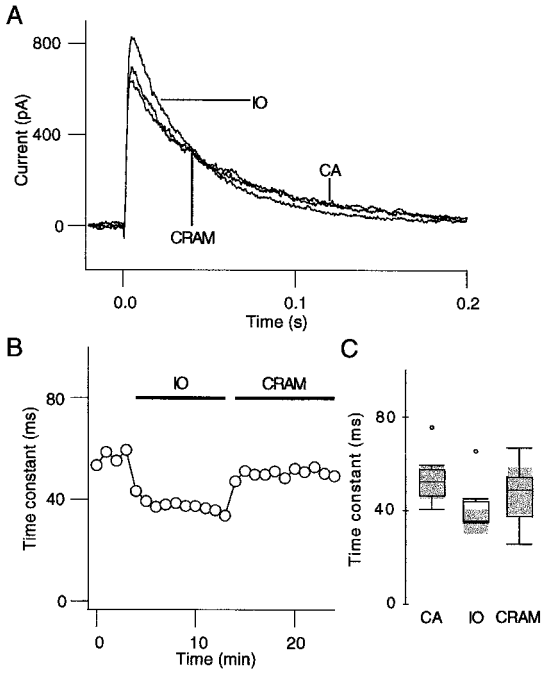

FIGURE 9 The inactivation time course of the ShBΔ6–46:M440L:T449S channel is less sensitive to patch excision. (*A*) Representative currents recorded in response to pulses from −90 mV to +50 mV in the cell-attached (CA), inside-out (IO), and cramming (CRAM) configurations in one experiment. (*B*) The currents traces from the experiment shown in *A* were fitted with a single exponential, and the time constant value is plotted as a function of time. The patch-clamp configurations are indicated by the horizontal bars. (*C*) The current traces from multiple patches (n = 7) are fitted with a single exponential, and the time constant values are compared using box plots.

To test this hypothesis, we mutated M440 to L, which is less readily oxidized than methionine (Stadtman, 1993; Vogt, 1995). In the ShBΔ6–46:T449K background, mutation of M440 to I is known to accelerate the inactivation time course (Schlief et al., 1996). Representative macroscopic currents from the ShBΔ6–46:M440L:T449S channels recorded are shown in Fig. 9 *A*. Unlike the inactivation time course of the ShBΔ6–46:T449S channel, that of the ShBΔ6–46:M440L:T449S channel was consistent among the patches examined. Furthermore, the ShBΔ6–46:M440L:T449S inactivation time course was well described by a single exponential whose time constant value, ~60–80 ms (Fig. 9 *B*), was similar to that of the slow exponential component in the ShBΔ6–46:T449S channel (see Fig. 2). Representative ShBΔ6–46:M440L:T449S currents recorded in the three patch-clamp configurations are shown in Fig. 9 *A*. Patch excision slightly accelerated the inactivation time course and unexpectedly enhanced the peak current amplitude. However, unlike the effect of patch excision observed on the ShBΔ6–46:T449S channel, these effects were fully reversible upon patch cramming (Fig. 9 *B*). The inactivation time constant values obtained from multiple patches in the cell-attached, inside-out, and cramming configurations are compared in Fig. 9 *C*. The difference in the mean time constant value between the cell-attached and inside-out configurations was significant (p = 0.0136, paired t-test). However, the difference between the cell-attached and cramming configurations was not significant (p = 0.3085, paired t-test), confirming the full reversibility. This observation indicates that M440 may be responsible in part for the effect by patch excision of accelerating the inactivation time course of the ShBΔ6–46:T449S channel.

We also tested the sensitivity of the ShBΔ6–46:M440L:T449S channel to H_2O_2 and found that H_2O_2 (up to 0.3%) did not alter the channel inactivation time course (Fig. 10). The inactivation time constant values estimated before and after H_2O_2 application are compared in Fig. 10 *C,* using box plots, showing the lack of the H_2O_2-sensitivity of this channel. H_2O_2, however, slightly increased the peak current amplitude in many patches. Furthermore, high O_2, which accelerated the ShBΔ6–46:T449S inactivation time course (see Fig. 7), failed to affect the inactivation time course of the channel in a noticeable manner (Fig. 11). As with H_2O_2, high O_2 slightly increased the peak current amplitude. These results further suggest that the effects of patch excision, H_2O_2, and O_2 observed in the ShBΔ6–46:T449S channel

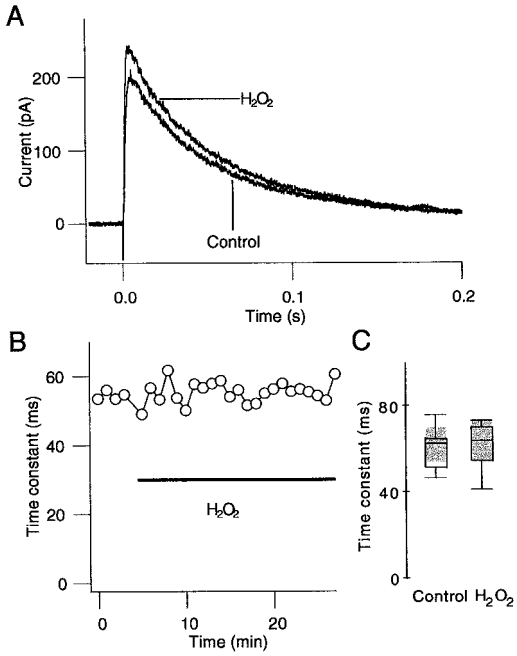

FIGURE 10 H_2O_2 does not alter the inactivation time course of the ShBΔ6–46:M440L:T449S channel. (*A*) Representative currents recorded in response to pulses from −90 mV to +50 mV in the cell-attached configuration before and after H_2O_2 (0.3%). (*B*) The current traces from the experiment shown in *A* were fitted with a single exponential, and the time constant value is plotted as a function of time. The H_2O_2 application period is indicated by the dark horizontal bar. 0.1% H_2O_2 was applied for 10 min, and then 0.3% was applied thereafter. Note that 0.3% is greater than the concentration required to accelerate the inactivation time course of the ShBΔ6–46:T449S channel (see Fig. 6). (*C*) Inactivation time constant values at +50 mV from multiple patches ($n = 7$) measured before and after H_2O_2 (≥0.1%) are compared using box plots.

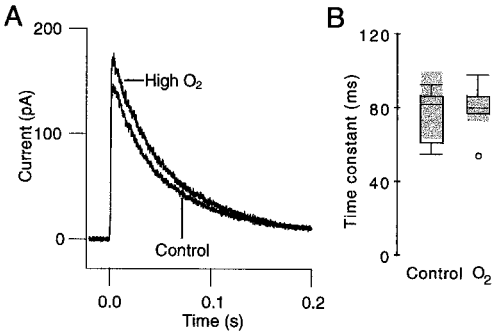

FIGURE 11 High O_2 does not alter the inactivation time course of the ShBΔ6–46:M440L:T449S channel. (*A*) Representative currents recorded in response to pulses from −90 mV to +50 mV in the cell-attached configuration before and after application of the high O_2 solution. The normal bath solution, aerated with 100% O_2 for at least 20 min, was applied (three times the bath volume) every 4 min. The current shown was recorded 14 min after application of the high-O_2 solution. (*B*) The current traces from multiple experiments ($n = 5$) were fitted with a single exponential, and the time constant values before and after high O_2 application are compared using box plots.

may be mediated at least in part by oxidation of methionine at position 440 in the P-segment. Because patch excision and oxidation are expected to have multitudes of effects, we cannot totally exclude the possibility that other effects contribute to the observed acceleration of the inactivation time course.

Conformational changes associated with channel gating are known to regulate accessibility/reactivity of the amino acid residues in the channel protein, so that state-dependent modifications of the channel function may be achieved (for a review, see Yellen, 1998). We considered the possibility that regulation of the inactivation time course by patch excision, which is probably mediated by oxidation of M440 in the P-segment (see above), is dependent on the channel opening. It might be expected that opening of the activation gate may increase the accessibility of M440. Thus we tested whether the depolarization pulse frequency affected the efficacy of patch excision in accelerating the inactivation time course. Immediately after the patch excision, the patch was held at −120 to −140 mV without any depolarizing pulse to prevent the channels from opening for 10 min. After this hyperpolarization period, depolarizing pulses were applied every 60 s. Although in a few cases this protocol clearly prevented the acceleration of the inactivation time course in ShBΔ6–46:T449S by patch excision or H_2O_2, the results were too inconsistent to firmly support the hypothesis.

MSRA catalyzes reduction of met(O) to methionine by using cellular thioredoxin or dithiothreitol (DTT) in vitro (Rahman et al., 1992; Moskovitz et al., 1996). Application of DTT alone (1 mM) to the cytoplasmic side of the inside-out patch did not have any detectable effect on the inactivation time course of the ShBΔ6–46:T449S channel ($n = 3$). The failure of DTT alone to reverse the acceleration of P/C-type inactivation further argues against involvement of disulfide bridge formation. We applied purified recombinant bovine MSRA (0.06 μg/μl) (Moskovitz et al., 1996) to the ShBΔ6–46:T449S channel in the presence of DTT (1 mM). This condition has been shown to reduce the oxidized methionine in the ShC/B inactivation peptide to methionine (Ciorba et al., 1997). Incubation with MSRA and DTT for up to 20 min did not noticeably affect the ShBΔ6–46:T449S inactivation time course in the inside-out configuration ($n = 4$).

DISCUSSION

We show here that patch excision accelerates P/C-type inactivation of the ShBΔ6–46:T449S channel that lacks the ball-and-chain N-type inactivation by decreasing the fractional amplitude of the slow inactivation component. The physiological oxidants, H_2O_2 and O_2, also accelerate the inactivation time course in a kinetically similar manner. The mutagenesis results suggest that this acceleration of P/C-type inactivation is mediated at least in part by oxidation of

a methionine residue (M440) located in the P-segment of the channel.

Double-exponential inactivation time course of ShBΔ6–46:T449S

The double-exponential inactivation time course in the absence of N-type inactivation was noted by López-Barneo et al. (1993) in ShBΔ6–46:T449T, where a very small fast inactivation component was observed in addition to the main slow inactivation component, although this small fraction was not included in the analysis (López-Barneo et al., 1993). In the ShBΔ6–46:T449S channel, the double-exponential nature is much more noticeable, with the slow inactivation component accounting for 30–50%, depending on the external K^+ (Figs. 2 and 5). These two components are observed using both low and high external K^+, although the relative amplitude of the slow component is greater with high K^+ (see Figs. 2 and 5). By manipulating hydrostatic pressure, Meyer and Heinemann (1997) showed that the ShBΔ6–46:T449S channel shows two distinct inactivation phases and that the inactivated state has a smaller volume. They further showed that the time course of recovery from inactivation, in contrast, is described by a single exponential. At the moment, it is not clear what molecular mechanisms underlie the two inactivation components. The ShB channel without N-type inactivation undergoes two additional experimentally distinguishable inactivation processes, P- and C-type inactivation (Cha and Bezanilla, 1997; Meyer and Heinemann, 1997; Olcese et al., 1997; Loots and Isacoff, 1998). Loots and Isacoff (1998) further suggested that the Shaker channel sequentially enters the P-type inactivated state, which is relatively unstable, and then the stable C-type inactivated state. This interpretation can be kinetically described by the linear three-state model presented earlier (Scheme II) that predicts the presence of two exponential components. The T449S mutation may alter the rate constants involved in P/C-type inactivation such that the two inactivation processes become better separated in time, so that these components are more visible in ShBΔ6–46:T449S than in ShBΔ6–46:T449K or ShBΔ6–46:T449T.

K^+ channel inactivation and patch excision

Inactivation of voltage-gated K^+ channels is often labile and subject to regulation by patch excision. The N-terminal cysteine residues in Kv1.4 and Kvβ are quite sensitive to oxidation (Ruppersberg et al., 1991; Rettig et al., 1994; Heinemann et al., 1995). Patch excision to separate the channel from the reduction-promoting cell interior readily slows the N-type inactivation time course. A critical methionine residue in the N-terminal ball domain of the ShC/B channel is also oxidized by patch excision, slowing the overall inactivation time course (Ciorba et al., 1997). These N-terminal residues may be particularly vulnerable to oxidation because the channel N-terminus does not form a well-defined structure, and these amino acid residues may be exposed to various oxidants. Kupper et al. (1995) showed that patch excision also accelerated P/C-type inactivation time course in the Kv1.3 channel. They also showed that the acceleration is not dependent on the protein kinase A or C phosphorylation consensus sequences. We showed here that patch excision, H_2O_2, and O_2 accelerated the inactivation time course in a very similar manner. The M440L mutation largely eliminated the sensitivities to these experimental treatments. These results thus indicate that oxidation of methionine at position 440 in ShB may be at least partially responsible for the acceleration of P/C-type inactivation observed on patch excision in some channels. Our results also confirm the conclusion of Kupper et al. (1995) that PKA- or PKC-mediated phosphorylation is not involved. It is possible, however, that the M440L mutation acts indirectly to modulate the patch excision and oxidation sensitivity of another amino acid located elsewhere. The results presented do not totally exclude this possibility. Another methionine in the P-segment is also important to the channel's sensitivity to oxidation induced by Ch-T, which readily oxidizes methionine and cysteine (Schlief et al., 1996). In the presence of Ch-T, the inactivation time course becomes faster and the rundown process is accelerated. Shlief et al. further showed that M448 located in the external mouth of the pore may participate in mediating this effect of Ch-T. It is possible that oxidation of both M440 and M448 may work through the same underlying mechanism (see below). Given the interpretation that oxidation of M440 may be responsible for this kinetic change, the results indicate that M440 is very readily oxidized. Considering the putative location of M440 (see below), this high oxidation susceptibility of M440 is somewhat surprising.

Oxidation of M440

Doyle et al. reported the crystal structure of a bacterial channel (KcsA), which is similar to the P-segment of the Shaker channel (Doyle et al., 1998). It is likely that the structure of the ShBΔ6–46:T449S channel is comparable to the KcsA structure (Fig. 12). At least in calmodulin, oxidation of multiple methionine residues leads only to local structural changes (Gao et al., 1998). Based on the KcsA crystal structure, the M440 residue is located near the large water-filled cavity of the channel cytoplasmic to the putative selectivity filter. The activation gate of the channel is considered to be located at the cytoplasmic side of this aqueous cavity (Liu et al., 1997). Furthermore, according to the same structure, the side chain of the M440 residue projects away from the pore, and it is located within several Å of the A463 residue in the S6-segment. Position 463 has been shown to affect P/C-type inactivation in the ShB channel (Hoshi et al., 1991; López-Barneo et al., 1993), in part by changing the K^+ affinity (Ogielska and Aldrich,

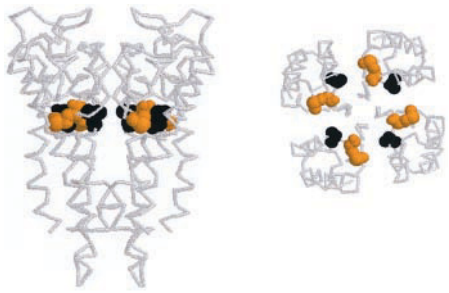

FIGURE 12 The putative structure of the S5-, P-, and S6-segments of the Shaker channel. Based on the sequence alignment between ShB and KcsA, the structure reported by Doyle et al. (1998) was adopted for the ShB channel. The left panel shows the side view of the channel, and the right panel shows the channel viewed from the cytoplasmic side sliced at the A463 residue level. The M440 residues are show in yellow, and the A463 residues are shown in black. The images were created with RasMol (http://www.umass.edu/microbio/rasmol/), using the method of Guex and Pietsch (1997).

1998). The extent by which the 463 residue influences the inactivation time course is critically dependent on the amino acid at position 449 in the external mouth of the pore (López-Barneo et al., 1993), which may be located just external to the C-type inactivation gate (Molina et al., 1997). When a threonine is present at position 449, mutations at position 463 markedly influence the inactivation kinetics, and the influence is much diminished when a tyrosine or valine is present at position 449 (Hoshi et al., 1991; López-Barneo et al., 1993). How these two residues interact to determine the inactivation time course is not known, although direct side-chain interactions are considered unlikely because of their putative distant three-dimensional locations (Ogielska et al., 1995). Because patch excision, H_2O_2, and O_2 work in a similar way by decreasing the fractional amplitude of the slow inactivation and substitution of a methionine at position 440 with a leucine, which is oxidized less readily, and this effect is abolished by methionine, we conclude that oxidation of M440 to met(O) is responsible at least in part for the observed acceleration of the inactivation time course. Based on the potential structural proximity between M440 and A463, we suggest that oxidation of M440 to met(O), as induced by patch excision, H_2O_2, and O_2, alters P/C-type inactivation via the A463 residue in the S6-segment. Oxidation of methionine essentially converts the nonpolar side chain to a hydrophilic group by adding an oxygen to the sulfur atom (Vogt, 1995). The hydrophobicity of met(O) is estimated to be similar to that of lysine (Black and Mould, 1991; Black, 1992), and if met(O) is oxidized to methionine sulfone, the hydrophobicity is further reduced (Black, 1992). It is plausible that this change at position 440 influences the A463 residue, which in turn regulates the inactivation time course. Kinetic analysis of the single-channel and macroscopic data suggests that those states involved in the burst behavior are destabilized by oxidation of M440, and this may alter the influence of the A463 residue on the channel inactivation gating. Mutations of the A463 residue have been shown to alter the open and burst durations (Avdonin et al., 1997). If we assume that the double-exponential nature of the ShBΔ6–46:T449S inactivation (this study; Meyer and Heinemann, 1997) reflects the sequential transition of the channel into the P- and then C-type inactivated states, as suggested (Loots and Isacoff, 1998) and represented in Scheme II, the results presented here indicate that oxidation of M440 to met(O) preferentially promotes the channel's transition into the P-type inactivated state without noticeably affecting the transition from the P-type inactivated state to the C-type inactivated state. In contrast, our results suggest that the time course of recovery from P- and C-type inactivation in the ShBΔ6–46:T449S channel is not markedly altered by patch excision and oxidation. This observation is in line with the conclusion of Meyer and Heinemann that there is only one rate-limiting step in the recovery process (Meyer and Heinemann, 1997).

High external K^+ slows down P/C-type inactivation (López-Barneo et al., 1993; Baukrowitz and Yellen, 1995; Levy and Deutsch, 1996; Starkus et al., 1997), and the A463C mutation influences the K^+ sensitivity (Ogielska and Aldrich, 1999). It is not likely, however, that oxidation of M440 exerts its effect on the inactivation time course by decreasing the ShBΔ6–46:T449S channel's affinity to K^+ ions, because very similar acceleration was observed in the presence of both 10 and 140 mM extracellular K^+. With high external K^+, the ion binding site(s) responsible for slowing of the inactivation process may be maximally occupied, and changes in the K^+ affinity are expected to have fewer noticeable effects on the inactivation time course.

The ShB M440 residue is well conserved in a variety of voltage-gated K^+ channels, especially in the Kv1 family, including Kv1.3. However, oxidation-induced regulation is not observed in every K^+ channel with a methionine at the equivalent position. For example, in the Kv1.3 channel, mutation of the ShB T449 equivalent amino acid to a tyrosine slowed P/C-type inactivation and reduced the patch excision sensitivity (Kupper et al., 1995). Given that M440 may exert its action via residue 463 (see above), this may not be surprising if one considers the results that the influence of residue 463 is dependent on the amino acid at position 449 (Hoshi et al., 1991; López-Barneo et al., 1993). For example, residue 463 does not appreciably alter the inactivation time course when a tyrosine or valine is present at position 449. The interaction between residues 449 and 463 may be partly explained by the observation that the effect of oxidation induced by Ch-T on the Shaker channel is not markedly dependent on M440 (Schlief et al., 1996). The results in this study suggest that, with a serine present at position 449, the 463 residue plays a dominant role in determining the inactivation time course, most likely by accelerating the transition from the open state to the P-type

inactivated state, which can be regulated by oxidation of methionine to met(O) at position 440.

The results of the holding voltage manipulation to test the hypothesis that acceleration of P/C-type inactivation by patch excision or H_2O_2 is prevented if the channel is kept closed were inconsistent and failed to directly support the hypothesis. Oxidants like H_2O_2 are small and may access the M440 residue located in the cavity inside of the putative activation gate whether it is closed or open. Assuming that the ShB structure is similar to that of KcsA reported by Doyle et al. (1998), the sulfur atom of M440 is not readily accessible from the cytoplasmic side by large molecules (see Fig. 12). Considering this putative location of the M440 residue, it is not surprising that acutely applied MSRA from the cytoplasmic side did not restore the inactivation time course of the ShBΔ6–46:T449S channel.

Methionine oxidation as a regulator of cellular excitability

Many biological oxidants, such as hydrogen peroxide, hydroxyl radical, hypochlorous acid, and chloramine, oxidize methionine to met(O) (Vogt, 1995). An increasing number of reports indicate that oxidation of methionine residues in proteins has marked functional consequences (Ciorba et al., 1997, 1999; Berlett et al., 1998; Gao et al., 1998), some of which can be reversed by exogenous MSRA (Ciorba et al., 1997, 1999; Kuschel et al., 1999). Dual roles of methionine oxidation and MSRA, as a tissue repair mechanism and as a cellular function regulator, have been proposed (Levine et al., 1996; Ciorba et al., 1997, 1999; Berlett et al., 1998; Gao et al., 1998; Moskovitz et al., 1998; Kuschel et al., 1999). Exactly how and which protein functions are altered depends on many factors, including the accessibility of the critical methionine residues. Naturally, the exposed residues are more likely to be oxidized, as found in the Shaker channel N-terminus (Ciorba et al., 1997, 1999; Kuschel et al., 1999). In calmodulin, methionine oxidation inhibits its activation of the plasma membrane Ca-ATPase (Yao et al., 1996), and the susceptibility of methionine to oxidation is directly related to the solvent exposure (Gao et al., 1998). In addition, localization of the target proteins with oxidant-generating elements may also confer specificity of the methionine oxidation action. For example, colocalization with nitric oxide synthase (Brenman et al., 1996a,b) may render some proteins particularly susceptible to oxidation. Although not yet reported, possible subcellular localization of MSRA, perhaps in association with other regulatory proteins, could bring about additional regulatory potential. Functional modifications of many proteins by methionine oxidation listed above and differential distributions of MSRA in different tissues (Kuschel et al., 1999) suggest that methionine oxidation and MSRA may have important physiological roles and that dysfunction of MSRA may underlie some pathological conditions.

We thank Dr. J. Thommandru, M. Masropour, and A. Freet for technical assistance and M. Sharp for spectral ideas.

This work was supported in part by the National Institutes of Health (GM57654) and DFG He2993/1.

REFERENCES

Avdonin, V., E. Shibata, and T. Hoshi. 1997. Dihydropyridine action on voltage-dependent potassium channels expressed in *Xenopus* oocytes. *J. Gen. Physiol.* 109:169–180.

Baukrowitz, T., and G. Yellen. 1995. Modulation of K^+ current by frequency and external $[K^+]$: a tale of two inactivation mechanisms. *Neuron.* 15:951–960.

Berlett, B. S., R. L. Levine, and E. R. Stadtman. 1998. Carbon dioxide stimulates peroxynitrite-mediated nitration of tyrosine residues and inhibits oxidation of methionine residues of glutamine synthetase—both modifications mimic effects of adenylation. *Proc. Natl. Acad. Sci. USA.* 95:2784–2789.

Black, S. D. 1992. Development of hydrophobicity parameters for prenylated proteins. *Biochem. Biophys. Res. Commun.* 186:1437–1442.

Black, S. D., and D. R. Mould. 1991. Development of hydrophobicity parameters to analyze proteins which bear post- or cotranslational modifications. *Anal. Biochem.* 193:72–82.

Brenman, J. E., D. S. Chao, S. H. Gee, A. W. McGee, S. E. Craven, D. R. Santillano, Z. Wu, F. Huang, H. Xia, M. F. Peters, S. C. Froehner, and D. S. Bredt. 1996a. Interaction of nitric oxide synthase with the postsynaptic density protein PSD-95 and alpha1-syntrophin mediated by PDZ domains. *Cell.* 84:757–767.

Brenman, J. E., K. S. Christopherson, S. E. Craven, A. W. McGee, and D. S. Bredt. 1996b. Cloning and characterization of postsynaptic density 93, a nitric oxide synthase interacting protein. *J. Neurosci.* 16: 7407–7415.

Cha, A., and F. Bezanilla. 1997. Characterizing voltage-dependent conformational changes in the Shaker K^+ channel with fluorescence. *Neuron.* 19:1127–1140.

Chance, B., H. Sies, and A. Boveris. 1979. Hydroperoxide metabolism in mammalian organs. *Physiol. Rev.* 59:527–605.

Chao, C. C., Y. S. Ma, and E. R. Stadtman. 1997. Modification of protein surface hydrophobicity and methionine oxidation by oxidative systems. *Proc. Natl. Acad. Sci. USA.* 94:2969–2974.

Ciorba, M. A., S. H. Heinemann, H. Weissbach, N. Brot, and T. Hoshi. 1997. Modulation of potassium channel function by methionine oxidation and reduction. *Proc. Natl. Acad. Sci. USA.* 94:9932–9937.

Ciorba, M. A., S. H. Heinemann, H. Wessbach, N. Brot, and T. Hoshi. 1999. Regulation of voltage-dependent K^+ channels by methionine oxidation: effect of nitric oxide and vitamin C. *FEBS Lett.* 442:48–52.

Doyle, D. A., J. M. Cabral, R. A. Pfuetzner, A. L. Kuo, J. M. Gulbis, S. L. Cohen, B. T. Chait, and R. Mackinnon. 1998. The structure of the potassium channel—molecular basis of K^+ conduction and selectivity. *Science.* 280:69–77.

Duprat, F., E. Guillemare, G. Romey, M. Fink, F. Lesage, M. Lazdunski, and E. Honore. 1995. Susceptibility of cloned K^+ channels to reactive oxygen species. *Proc. Natl. Acad. Sci. USA.* 92:11796–11800.

Gao, J., D. H. Yin, Y. H. Yao, H. Y. Sun, Z. H. Qin, C. Schoneich, T. D. Williams, and T. C. Squier. 1998. Loss of conformational stability in calmodulin upon methionine oxidation. *Biophys. J.* 74:1115–1134.

Guex, N., and M. C. Peitsch. 1997. SWISS-MODEL and the Swiss-PdbViewer: an environment for comparative protein modeling. *Electrophoresis.* 18:2714–2723.

Heginbotham, L., Z. Lu, T. Abramson, and R. MacKinnon. 1994. Mutations in the K^+ channel signature sequence. *Biophys. J.* 66:1061–1067.

Heinemann, S. H., J. Rettig, F. Wunder, and O. Pongs. 1995. Molecular and functional characterization of a rat brain Kvβ 3 potassium channel subunit. *FEBS Lett.* 377:383–389.

Hoshi, T., W. N. Zagotta, and R. W. Aldrich. 1990. Biophysical and molecular mechanisms of *Shaker* potassium channel inactivation. *Science.* 250:533–538.

Hoshi, T., W. N. Zagotta, and R. W. Aldrich. 1991. Two types of inactivation in *Shaker* K^+ channels: effects of alterations in the carboxy-terminal region. *Neuron.* 7:547–556.

Hoshi, T., W. N. Zagotta, and R. W. Aldrich. 1994. *Shaker* potassium channel gating. I. Transitions near the open state. *J. Gen. Physiol.* 103:249–278.

Iverson, L. E., and B. Rudy. 1990. The role of the divergent amino and carboxyl domains on the inactivation properties of potassium channels derived from the *Shaker* gene of *Drosophila. J. Neurosci.* 10:2903–2916.

Keck, R. G. 1996. The use of *t*-butyl hydroperoxide as a probe for methionine oxidation in proteins. *Anal. Biochem.* 236:56–62.

Kourie, J. I. 1998. Interaction of reactive oxygen species with ion transport mechanisms. *Am. J. Physiol.* 275:C1–C24.

Kramer, R. H. 1990. Patch cramming: monitoring intracellular messengers in intact cells with membrane patches containing detector ion channels. *Neuron.* 4:335–341.

Kupper, J., M. R. Bowlby, S. Marom, and I. B. Levitan. 1995. Intracellular and extracellular amino acids that influence C-type inactivation and its modulation in a voltage-dependent potassium channel. *Pflügers Arch.* 430:1–11.

Kuschel, L., A. Hansel, R. Schönherr, H. Weissbach, N. Brot, T. Hoshi, and S. H. Heinemann. 1999. Molecular cloning and functional expression of a human peptide methionine sulfoxide reductase (hMsrA). *FEBS Lett.* 456:17–21.

Levine, R. L., L. Mosoni, B. S. Berlett, and E. R. Stadtman. 1996. Methionine residues as endogenous antioxidants in proteins. *Proc. Natl. Acad. Sci. USA.* 93:15036–15040.

Levy, D. I., and C. Deutsch. 1996. Recovery from C-type inactivation is modulated by extracellular potassium. *Biophys. J.* 70:798–805.

Liu, Y., M. Holmgren, M. E. Jurman, and G. Yellen. 1997. Gated access to the pore of a voltage-dependent K^+ channel. *Neuron.* 19:175–184.

Liu, Y., M. E. Jurman, and G. Yellen. 1996. Dynamic rearrangement of the outer mouth of a K^+ channel during gating. *Neuron.* 16:859–867.

Loots, E., and E. Y. Isacoff. 1998. Protein rearrangements underlying slow inactivation of the Shaker K^+ channel. *J. Gen. Physiol.* 112:377–389.

López-Barneo, J. 1996. Oxygen-sensing by ion channels and the regulation of cellular functions. *Trends Neurosci.* 19:435–440.

López-Barneo, J., T. Hoshi, S. H. Heinemann, and R. W. Aldrich. 1993. Effects of external cations and mutations in the pore region on C-type inactivation of *Shaker* potassium channels. *Receptors Channels.* 1:61–71.

Meyer, R., and S. H. Heinemann. 1997. Temperature and pressure dependence of Shaker K^+ channel N- and C-type inactivation. *Eur. Biophys. J.* 26:433–445.

Michaelis, M. L., D. J. Bigelow, C. Schoneich, T. D. Williams, L. Ramonda, D. Yin, A. F. Huhmer, Y. Yao, J. Gao, and T. C. Squier. 1996. Decreased plasma membrane calcium transport activity in aging brain. *Life Sci.* 59:405–412.

Molina, A., A. G. Castellano, and J. Lopez-Barneo. 1997. Pore mutations in Shaker K^+ channels distinguish between the sites of tetraethylammonium blockade and C-type inactivation. *J. Physiol. (Lond.).* 499:361–367.

Moskovitz, J., E. Flescher, B. S. Berlett, J. Azare, J. M. Poston, and E. R. Stadtman. 1998. Overexpression of peptide-methionine sulfoxide reductase in *Saccharomyces cerevisiae* and human T cells provides them with high resistance to oxidative stress. *Proc. Natl. Acad. Sci. USA.* 95: 14071–14075.

Moskovitz, J., H. Weissbach, and N. Brot. 1996. Cloning and expression of a mammalian gene involved in the reduction of methionine sulfoxide residues in proteins. *Proc. Natl. Acad. Sci. USA.* 93:2095–2099.

Ogielska, E. M., and R. W. Aldrich. 1998. A mutation in S6 of Shaker potassium channels decreases the K^+ affinity of an ion binding site revealing ion-ion interactions in the pore. *J. Gen. Physiol.* 112:243–257.

Ogielska, E. M., and R. W. Aldrich. 1999. Functional consequences of a decreased potassium affinity in a potassium channel pore-ion interactions and C-type inactivation. *J. Gen. Physiol.* 113:347–358.

Ogielska, E. M., W. N. Zagotta, T. Hoshi, S. H. Heinemann, J. Haab, and R. W. Aldrich. 1995. Cooperative subunit interactions in C-type inactivation of K channels. *Biophys. J.* 69:2449–2457.

Olcese, R., R. Latorre, L. Toro, F. Bezanilla, and E. Stefani. 1997. Correlation between charge movement and ionic current during slow inactivation in Shaker K^+ channels. *J. Gen. Physiol.* 110:579–589.

Rahman, M. A., H. Nelson, H. Weissbach, and N. Brot. 1992. Cloning, sequencing, and expression of the *Escherichia coli* peptide methionine sulfoxide reductase gene. *J. Biol. Chem.* 267:15549–15551.

Rettig, J., S. H. Heinemann, F. Wunder, C. Lorra, D. N. Parcej, J. O. Dolly, and O. Pongs. 1994. Inactivation properties of voltage-gated K^+ channels altered by presence of β-subunit. *Nature.* 369:289–294.

Ruppersberg, J. P., M. Stocker, O. Pongs, S. H. Heinemann, R. Frank, and M. Koenen. 1991. Regulation of fast inactivation of cloned mammalian IK(A) channels by cysteine oxidation. *Nature.* 352:711–714.

Schlief, T., R. Schönherr, and S. H. Heinemann. 1996. Modification of C-type inactivating Shaker potassium channels by chloramine-T. *Pflügers Arch.* 431:483–493.

Stadtman, E. R. 1993. Oxidation of free amino acids and amino acid residues in proteins by radiolysis and by metal-catalyzed reactions. *Annu. Rev. Biochem.* 62:797–821.

Starkus, J. G., L. Kuschel, M. D. Rayner, and S. H. Heinemann. 1997. Ion conduction through C-type inactivated Shaker channels. *J. Gen. Physiol.* 110:539–550.

Stephens, G. J., D. G. Owen, and B. Robertson. 1996. Cysteine-modifying reagents alter the gating of the rat cloned potassium channel Kv1.4. *Pflügers Arch.* 431:435–442.

Suzuki, Y. J., H. J. Forman, and A. Sevanian. 1997. Oxidants as stimulators of signal transduction. *Free Radic. Biol. Med.* 22:269–285.

Szabo, I., B. Nilius, X. F. Zhang, A. E. Busch, E. Gulbins, H. Suessbrich, and F. Lang. 1997. Inhibitory effects of oxidants on N-type K^+ channels in T lymphocytes and *Xenopus* oocytes. *Pflügers Arch.* 433:626–632.

Taglialatela, M., P. Castaldo, S. Iossa, A. Pannaccione, A. Fresi, E. Ficker, and L. Annunziato. 1997. Regulation of the human *ether-a-gogo* related gene (HERG) K^+ channels by reactive oxygen species. *Proc. Natl. Acad. Sci. USA.* 94:11698–11703.

Vega-Saenz de Miera, E., and B. Rudy. 1992. Modulation of K^+ channels by hydrogen peroxide. *Biochem. Biophys. Res. Commun.* 186: 1681–1687.

Velleman, P. F., and D. C. Hoaglin. 1981. Applications, Basics, and Computing of Exploratory Data Analysis. Duxbury, Boston.

Vogt, W. 1995. Oxidation of methionyl residues in proteins: tools, targets and reversal. *Free Radic. Biol. Med.* 18:93–105.

Wang, D., C. Youngson, V. Wong, H. Yeger, M. C. Dinauer, E. Vega-Saenz Miera, B. Rudy, and E. Cutz. 1996. NADPH-oxidase and a hydrogen peroxide-sensitive K^+ channel may function as an oxygen sensor complex in airway chemoreceptors and small cell lung carcinoma cell lines. *Proc. Natl. Acad. Sci. USA.* 93:13182–13187.

Wolin, M. S., and K. M. Mohazzab. 1997. Mediation of signal transduction by oxidants. *In* Oxidative Stress and the Molecular Biology of Antioxidant Defenses. J. G. Scandalios, editor. Cold Spring Harbor Laboratory, Cold Spring Harbor, NY. 21–48.

Yang, Y., Y. Yan, and F. J. Sigworth. 1997. How does the W434F mutation block current in Shaker potassium channels? *J. Gen. Physiol.* 109: 779–789.

Yao, Y., D. Yin, G. S. Jas, K. Kuczer, T. D. Williams, C. Schoneich, and T. C. Squier. 1996. Oxidative modification of a carboxyl-terminal vicinal methionine in calmodulin by hydrogen peroxide inhibits calmodulin-dependent activation of the plasma membrane Ca-ATPase. *Biochemistry.* 35:2767–2787.

Yellen, G. 1998. The moving parts of voltage-gated ion channels. *Q. Rev. Biophys.* 31:239–296.

Yellen, G., D. Sodickson, T. Y. Chen, and M. E. Jurman. 1994. An engineered cysteine in the external mouth of a K^+ channel allows inactivation to be modulated by metal binding. *Biophys. J.* 66: 1068–1075.

Zagotta, W. N., T. Hoshi, and R. W. Aldrich. 1989. Gating of single Shaker potassium channels in *Drosophila* muscle and in *Xenopus* oocytes injected with *Shaker* mRNA. *Proc. Natl. Acad. Sci. USA.* 86:7243–7247.